Distribution Agreement

In presenting this thesis as a partial fulfillment of the requirements for a degree from Emory University, I hereby grant to Emory University and its agents the non-exclusive license to archive, make accessible, and display my thesis in whole or in part in all forms of media, now or hereafter known, including display on the world wide web. I understand that I may select some access restrictions as part of the online submission of this thesis. I retain all ownership rights to the copyright of the thesis. I also retain the right to use in future works (such as articles or books) all or part of this thesis.

Signature:

_____	_____
Benjamin A. Kesler	April 19th, 2010

Combining Single Molecule Fluorescence and Force Experiments: Multiplexed Assays

by

Benjamin A. Kesler

Adviser: Dr. Ivan Rasnik

Department of Physics

_____

Dr. Ivan Rasnik
Adviser

_____

Dr. Jed Brody
Committee Member

_____

Dr. David Borthwick
Committee Member

_____

April 19th, 2010

Combining Single Molecule Fluorescence and Force Experiments: Multiplexed Assays

By

Benjamin A. Kesler

Adviser: Dr. Ivan Rasnik

An abstract of
A thesis submitted to the Faculty of Emory College of Arts and Sciences
of Emory University in partial fulfillment
of the requirements of the degree of
Bachelor of Sciences with Honors

Department of Physics

2010

Abstract

Combining Single Molecule Fluorescence and Force Experiments: Multiplexed Assays
By Benjamin A. Kesler

Single molecule fluorescence resonant energy transfer allows for following conformational changes of biomolecules in the sub-nanometer range with millisecond time resolution. The technique has been used to follow conformational dynamics of DNA and its interactions with DNA binding proteins *in vitro*. Inside the cell, DNA is physically constrained, so binding and translocation of proteins along the DNA result in application of torques and forces that may have an effect on its thermodynamic stability. It is important to understand the effect of physical constraints on the DNA because local conformation and flexibility of DNA have an effect in its interaction with proteins. Proof of principle type of experiments, in which DNA manipulation is combined with single molecule fluorescence detection, have been reported. In practice, the experiments are highly challenging from a technical point of view, limiting their scope of applications. In this work we improve and develop a series of techniques that allow generation of long DNA substrates (11 kbp in this case) with asymmetric ends for high yield/high efficiency selective labeling. Long DNA substrates with asymmetric ends were generated by over expression of plasmids in *E. coli.* Fragments were purified with high yields and adaptor DNA sequences attached selectively to the long DNA fragments using a low temperature ligation reaction compatible with long term stability of fluorescent dyes. To demonstrate high efficiency double-labeling of the long DNA fragments we specifically immobilized DNA on a microscope slide surface with a biotin/streptavidin linkage. The DNA free end was attached to antidigoxigenin coated polystyrene beads. Application of buffer at several flow rates was used to determine the yield of doubly-labeled substrates and to investigate the range of forces that can be applied with this scheme. Our results show that we can immobilize doubly-labeled substrates at high densities compatible with single molecule fluorescence observation and a large range of forces.

Combining Single Molecule Fluorescence and Force Experiments: Multiplexed Assays

By

Benjamin A. Kesler

Adviser: Dr. Ivan Rasnik

A thesis submitted to the Faculty of Emory College of Arts and Sciences
of Emory University in partial fulfillment
of the requirements of the degree of
Bachelor of Sciences with Honors

Department of Physics

2010

Acknowledgements

I would first like to thank Dr. Ivan Rasnik, because without him this project would not have been possible and I would not have been able to complete my thesis. He has been a great teacher and mentor throughout my time and Emory and I consider myself lucky to have studied and learned under his guidance.

Also, thank you Dr. Yuyen Lin (Kent) for helping me out for an entire year and teaching me all the things I never got a chance to learn about biology and chemistry. Without him this project would have been a disaster, with me unsure of what to do next or how to accomplish my goals. Thank you Julie Coats for the help you provided as well, and for making my time in the Rasnik lab enjoyable, even when the work days were long and tedious.

I would like to thank the entire physics and math department and Emory University for giving me the thirst for knowledge that has led me to continue my studies in the Electrical Engineering PhD program at the University of Illinois, specifically thanking Dr. Jed Brody and Dr. David Borthwick for serving on my honors committee.

Finally, I would like to thank my mother, Lydia, and my father, Morris, for giving love and support for my entire life (and for providing for my education here at Emory University), and my little sister, Sophia, who I know will go on to do great things in college and in life.

Table of Contents

List of Figures

List of Tables

Chapter 1

Introduction

1.1 Background

In the past few decades, the interest in single molecule manipulation experiments has increased exponentially since the advent of new technologies, such as ultra fast CCD cameras, that are able to accurately capture real time images of nanoscale proportions. Prior to this shift, most studies designed to collect data about molecular processes were evaluated using a macroscopic method known as ensemble averaging, a statistical technique that evaluates a system and draws conclusions about its behavior using the average of all molecules in that system. When the system is complex, as was generally the case when attempting to analyze molecular processes before the development of sufficiently precise equipment, ensemble averaging proves to be difficult to implement and solve. In fact, an ensemble average can not even apply forces or torques on molecules. This meant that though the basics of the DNA double helix were understood, direct measurements of its mechanical properties were impossible to make and the idea of observing individual DNA-protein interactions was nearly science fiction. Since then, however, the ability to manipulate single molecules with tremendous precision, along with calculating position measurements to angstrom level accuracy, has allowed scientists to gain considerable insight into the fundamental properties and processes that govern DNA and RNA functions, both internally and in the surrounding environment.

Some of the first single-molecule manipulation experiments revolved around characterizing the elastic properties of single and double stranded DNA (Smith, Finzi et al. 1992; Bustamante, Marko et al. 1994; Smith, Cui et al. 1996). In the years preceding these experiments, DNA had been theoretically viewed as an ideal or freely jointed chain, the most basic polymer model in polymer physics. The freely jointed chain model represents polymers as a random walk of equal length segments, flexible only at their connecting joints, and assumes that each segment, or monomer, acts independently of all others. Thus, the vast number of microscopic random walk states the segments can form describes the macroscopic state of the polymer. In the freely jointed chain model, as with all polymer models, the total and internal energy of the polymer are constant, meaning that if both ends are attached to an external device, any force exerted on the device is entropic and stretching the polymer results in a large decrease in entropy (Marko and Siggia 1995). DNA, as with any system that experiences entropic forces, is constantly looking to return to a macroscopic state representative of the maximum possible number of microscopic states. Thus, the stretching of a polymer produces a restoring force as the chain attempts to return to its equilibrium state, a trait DNA displays by coiling when in solution. This property of polymers is formally called entropic elasticity and experiments to determine the elastic properties and force-extension relationships of single DNA molecules comprise the vast majority of testing on general polymer entropic elasticity to date.

One of the first papers to experimentally attempt direct measurements of force versus extension for single DNA molecules was written in 1992 and utilized a combination of magnetic tweezers and hydrodynamic flow to apply well characterized forces on a paramagnetic bead attached to the free end of a tethered DNA strand (Smith, Finzi et al. 1992). The experimental data gathered was then plotted alongside the theoretical force extension curve predicted by the freely jointed chain model which, when fit to low-force data measurements, failed to accurately depict DNA extension for forces greater than 1pN and less than 10pN (Smith, Finzi et al. 1992).

In an attempt to explain this failure the paper theorized that the worm-like chain model, the second model in polymer physics, could better describe the force-extension relationship for DNA. However, the ability to treat DNA as a WLC had not been developed at the time, so the authors decided that the molecule would be best described as a combination of two separate FJC models that corresponded to high and low stretching forces (Smith, Finzi et al. 1992).

The authors, as it turns out, were correct in assuming that DNA can be modeled much more accurately as a worm-like chain. The WLC model is best for describing stiffer polymers such as DNA and differs from the FJC model in that it assumes the polymer to be a continuously flexible isotropic rod rather than a series of monomers that bend only at their joints. This flexibility is characterized by a single quantity known as the persistence length, defined as the distance of a line along which the direction of the polymer is maintained; beyond this distance the orientations of different polymer segments become less correlated. If we define θ to be the angle between two tangential vectors separated by a distance L and P to be the persistence length of the polymer it can be shown that the expectation value of cos(θ), essentially the correlation between segments, falls off exponentially with decay length P: $\langle \cos\theta \rangle = e^{-(L/P)}$. The numerical solution of the WLC model, which is complex to analyze and analogous to the quantum mechanical solution for a dipole in an electric field (Strick, Allemand et al. 2000), was solved in two landmark 1995 papers by Marko and Siggia (Marko and Siggia 1995). Those same papers also addressed the problem of self-avoidance, the idea that a randomly coiled polymer will swell to a larger size depending on its orientation and the fact that it cannot intersect itself. Though this phenomenon is a normal occurrence at equilibrium – due to thermal fluctuations and the fact that DNA is highly charged so segments repel one another – it could theoretically prove problematic to proper extension measurements if the end-to-end distance randomly fluctuates as the DNA is stretched. However, Marko and Siggia proved that for a random coil with an equilibrium end-to-end distance given by $R_0 = (2PL)^{1/2}$, where L is the contour length of the DNA, extension to

lengths of only a few times R_0 negates self-avoidance effects (Marko and Siggia 1995b). The idea that self-avoidance effects can be neglected was explored in depth a few years later and it was shown that self-avoidance becomes a factor if the contour length of the DNA in question is greater than 40μm (Strick, Allemand et al. 2000). However, nearly all DNA fragments that are used in force-extension experiments and single-molecule assays are of considerably smaller length, rendering these effects null. In the end, even though a segment reacts, albeit slightly, to the orientation of the connecting monomers, the total polymer length of a WLC can still be characterized by a truly random walk, just as in the FJC model.

Since the seminal 1995 papers were published the elasticity of both single and double stranded DNA has been extensively studied, confirming the WLC theory for ssDNA but producing startling results for dsDNA. To begin, single stranded DNA is inherently more flexible than double stranded DNA as it is not a double helix, giving it the ability to assume much more compact formations. As a result, when an external force of less than ~6pN (Bustamante, Bryant et al. 2003) is applied to a ssDNA molecule it produces a much smaller extension than if the same force was applied to a dsDNA molecule. At larger forces ssDNA molecules far outstretch their dsDNA counterparts becoming, as expected, nearly twice the contour length of the dsDNA, whose extension is limited by its double helix configuration. The WLC model for dsDNA predicts that the contour length can never be reached due to the infinite amount of force required to extend the molecule to that size (**Figure 1**). The following formula describes the force-extension relationship of a WLC in the entropic region (extension less than the contour length),

$$\frac{FP}{k_B T} = \frac{1}{4}\left(1 - \frac{x}{L_0}\right)^{-2} - \frac{1}{4} + \frac{x}{L_0} \qquad (1)$$

where k_B is the Boltzmann constant, P is the persistence length, x is the extension of the DNA, L_0 is the contour length, and T is the temperature. In the entropic region the stretching behavior of the DNA is assumed to be inextensible.

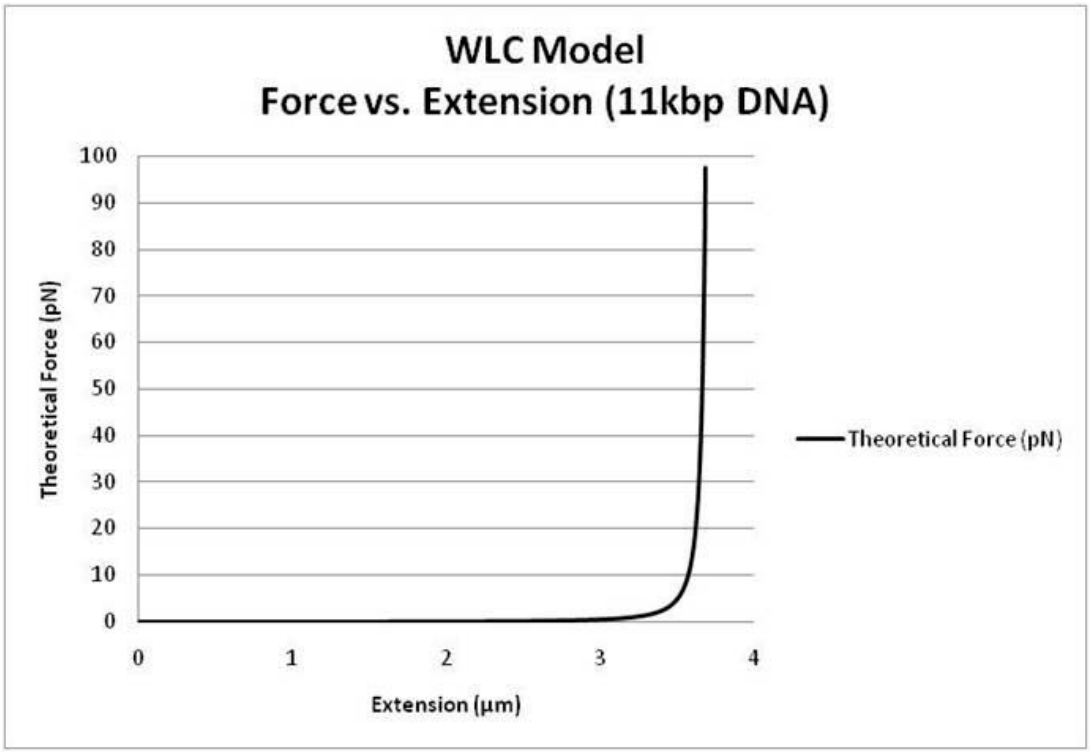

Figure 1: Theoretical force extension curve based on the worm-like chain (WLC) model of polymer physics, in this case for an 11kbp DNA strand. Force measurements can be compared to this model and other relations, such as flow rate versus extension, can be derived based on data plots.

Initial experiments confirmed that the extension of dsDNA did indeed approach a vertical asymptote at the contour length but that enthalpic stretching occurred in the region close (~10%) to the contour length. This stretching can be described by the following equation, which assumes the DNA in this region to be extensible,

$$\frac{x}{L_0} = 1 - \frac{1}{2}\left(\frac{k_B T}{FP}\right)^{1/2} + \frac{F}{S} \qquad (2)$$

When stretching forces in the enthalpic region exceeded ~70pN, dsDNA suddenly grew to a size 70% longer than its contour length (Cluzel, Lebrun et al. 1996; Smith, Cui et al. 1996),

an event known as overstretching and something that the WLC model had not predicted. The structure of this new form of DNA depended on which pair of asymmetric ends (3'-3' or 5'-5') was bound to the external stretching mechanism. If the 3' (terminal hydroxyl group) pair was attached, the dsDNA unwound to resemble a slightly twisted ladder; however, if the 5' (terminal phosphate group) extremities were attached, the dsDNA retained its double helix form (Cluzel, Lebrun et al. 1996; Lebrun and Lavery 1996).

With the experimental results confirming the accuracy of the WLC model for describing the force-extension relationship for single and double stranded DNA, research began on the mechanical properties of single DNA molecules as well as individual DNA-protein interactions. Studies using a number of different manipulation techniques were conducted on a wide range of topics including replication, supercoil states, enzyme transcription, and viral packaging, in many cases helping to resolve disconnects between theories and data collected by earlier bulk studies.

1.2 The Ultimate Goal: Combining smFRET and Force Experiments

Single molecule experiments can be divided into two main categories: Manipulation of molecules using force and torque (literally: force experiments) and fluorescence. Manipulation experiments attempt to simulate what the molecule experiences in the cell and how interactions and conditions can change the system. Applying forces helps to determine what, if any, conformations changes DNA experiences as the system changes. Fluorescence experiments use single molecule FRET, or fluorescence resonance energy transfer, to measure distance changes in the angstrom range, something that force experiments are simply not able to do. FRET is a technique that is used to observe interactions and conformational changes between molecules by monitoring the distance between two neighboring chromophore molecules (a donor, such as Cy3, and an acceptor, such as Cy5) (Clegg 2004). The evanescent field created by TIRFM raises the energy level of the donor

chromophore to an excited state, yet does not affect the acceptor chromophore. When the molecules are separated by a distances between 30-80Å, the range where FRET is most effective (Rasnik, Mckinney et al. 2005), the energy of the donor is nonradiatively transferred to the acceptor via an induced-dipole interaction, exciting the acceptor chromophore from its ground state(Clegg 2004)(Rasnik, Mckinney et al. 2005). The efficiency of the energy transfer is given by the equation $E = 1 / [1 + (r / R_0)^6]$, where r is the distance between the donor and acceptor and R_0 is the Förster distance of the donor/acceptor pair, the distance at which the energy transfer efficiency is 50% (not discussed). Looking at the equation, it is clear to see that as the distance between the donor/acceptor pair increases, the energy efficiency transfer decreases. Real time intensity measurements can be made to accurately calculate changes in distance between the donor/acceptor pair using the experimental energy efficiency transfer equation $E = I_A / (I_D + I_A)$, where I_A and I_D are the intensities of the acceptor and donor chromophores, respectively (Rasnik, Mckinney et al. 2005).

What fluorescence experiments gain in precision, they lose in the fact that they cannot apply external forces on the DNA being studied, having to be content with simply observing interactions. Therefore, the ultimate goal for single molecule experiments is the combination of fluorescence and force manipulation. Very few papers to date use both techniques simultaneously due to the difficulty of creating DNA strands that are properly double labeled with substrates for both smFRET and force manipulation. However, the combination would allow researchers to actively simulate what DNA experiences in the cell, yet record distance changes with angstrom level accuracy. The final molecule would have a chromophore labeled substrate attached to the surface and one end of the DNA molecule, while the free end will be attached for a bead to allow for the application for force and torque (**Figure 2**). The DNA and bead system act as a handle to pull on the choromophore substrate, stretching and twisting it. The force measurements can be compared to the curve in **Figure 1** to estimate the amount of force the DNA is experiencing.

Combining that knowledge with the smFRET measurements will give researchers an unprecedented look at DNA interactions.

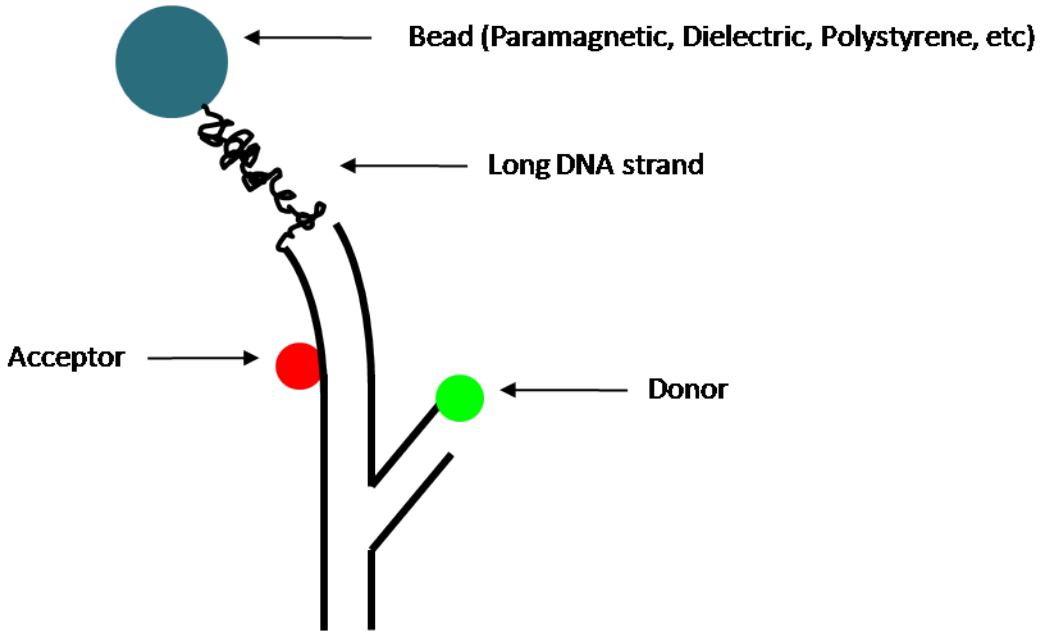

Figure 2: Schematic (not to scale) of what the smFRET and force manipulation DNA strand will look like. On one end is the chromophore labeled substrate, in this case a three way junction, and on the other is a bead on which forces can be applied. Distance changes in the angstrom region between the donor (green) and acceptor (red) chromophores can be measured, something force experiments alone cannot do.

1.3 Hydrodynamic and Electrophoretic Stretching

In equilibrium, long DNA strands configure themselves in the form of a coil that can be modeled by a random walk that assumes interaction between individual monomers. As mentioned earlier, the DNA can be divided into equal segments of length P, the persistence length, a quantity that measures the flexibility of long polymers, which has been independently shown for lambda DNA to equal approximately 50nm (Bustamante, Marko et al. 1994), 52 ± 2nm (Strick, Allemand et al. 2000), and 52.88 nm (Wang and Lu 2007). In this configuration the DNA has high conformational entropy representative of the vast number of possible random walk patterns. The work done on the system by the forces associated with the particular experimental technique that is used reduces the conformational entropy and stretches the DNA (Marko and Siggia 1995). The

stretching is opposed by an entropic force, a result of the DNA attempting to return to a macroscopic state that corresponds to a maximum number of microscopic configurations

Stretching using hydrodynamic flow is the result of drag forces due to liquid flow acting on the coiled DNA. Analysis of the force can be difficult due to the fact that the flow rate at each segment varies depending on the random position of all the other monomers (a condition of the WLC) (Stigter and Bustamante 1998) meaning that all random walk configurations must be considered in the calculations. Electrophoretic stretching is the result of an external electric field producing a force on the DNA proportional to its charge density, as well as from hydrodynamic and repulsive electric forces caused by the movement of ions in solution through and around the coils of the DNA. Since the force now depends on both hydrodynamics and the electric field interactions, analysis becomes even more difficult. A 1998 paper (Stigter and Bustamante 1998) expanded on the previously mentioned work of Bustamante and Marko (Bustamante, Marko et al. 1994)(Marko and Siggia 1995) and developed a rigorous statistical model for hydrodynamic flow that characterizes the sum of the frictional forces and tensions acting on each of these segments and relates them to the extension of the polymer. The paper also utilized the same model used for hydrodynamic stretching to derive a force equation for the more difficult case of electrophoretic stretching, which eliminated the problematic use of the charge density as an adjustable parameter in the Marko-Siggia equations (Marko and Siggia 1995), using the constant structural charge density of the DNA instead.

The experimental setup for hydrodynamic stretching is simple. The molecule being studied, usually DNA, is attached by one end to a bio-friendly surface such as a glass slide covered with either BSA (bovine serum albumin), PEG (polyethylene glycol), or a combination of the two in order to reduce or eliminate the number of nonspecific binding sites. The free end of the molecule can be bound to a polystyrene bead to increase the drag force and improve video imaging of the DNA. In fact, the geometric center of the bead can be located to within 1 nm

(Visnapuu, Duzdevich et al. 2008) using a technique known as centroid tracking, leading to precise length measurements. Because hydrodynamic stretching allows for such accurate measurements it is an ideal technique to observe DNA replication processes (Lee, Hite et al. 2006) or nucleic-acid enzyme detection (Kim, Blainey et al. 2007).

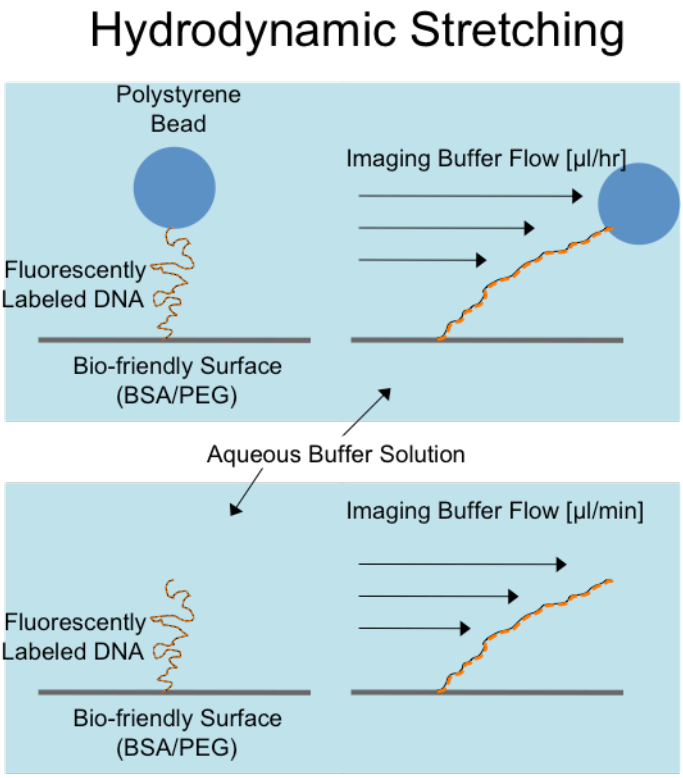

Figure 3: Hydrodynamic stretching is a commonly used single-molecule manipulation technique where the polymer in question (in this case, DNA) is attached at one end to a bio-friendly surface (BSA/PEG) while the other end is left free or attached to a polystyrene bead. Drag forces from buffer flow acting on the bead or molecule itself produce the stretching force.

Electrophoretic stretching is achieved by creating a large AC electric field, on the order of 10^6 V/m (Kim, Dukkipati et al. 2007), between microfabricated electrodes comprised commonly of gold. One end of the DNA is attached to the electrode and when the electric field materializes the DNA is immobilized across the gap through a combination of dielectric torque, which aligns the molecule, and field-induced flow forces that physically stretch the molecule. This rigid immobilization has been used to map specific DNA sequences that are detected by fluorescently tagged *Eco*RI enzymes, which are responsible for DNA integrity and slide up and

down the molecule, stopping when they reach their designated recognition sequence of GAATTC (Kabata, Okada et al. 2000).

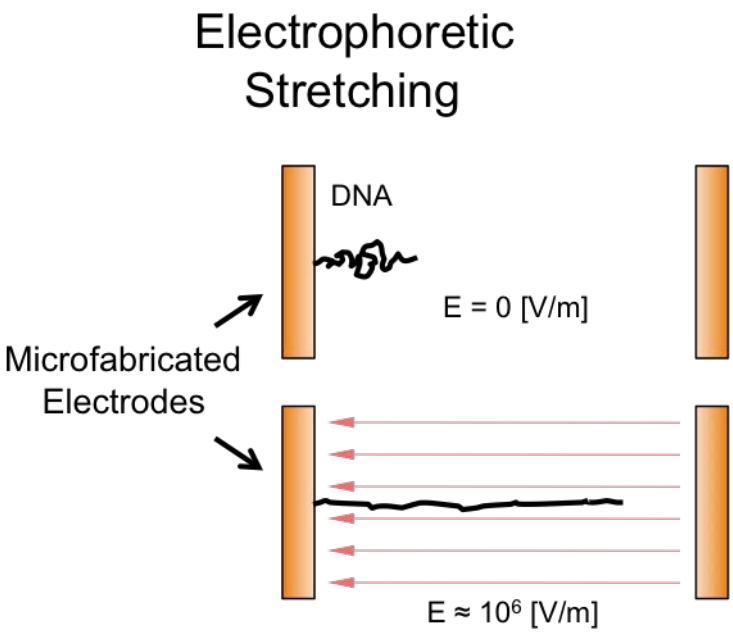

Figure 4: In electrophoretic stretching an electric field, on the order of 10^6V/m, is created between microfabricated electrodes (commonly comprised of gold). A DNA molecule, attached at one end in between the electrodes, is stretched to nearly its crystallized length.

1.4 Atomic Force Microscopy (AFM)

Atomic force microscopy, or AFM for short, is a scanning imaging technique that can generate a three dimensional profile of a surface using a cantilever with a probe attached at the end. The radius of curvature of the probe tip is very small, on the order of nanometers, and when it is brought close to a surface, forces between the sample and probe deflect the cantilever. This deflection is measured using a laser and a position-sensing detector normally consisting of separate photodiodes. The laser is reflected off the back of the cantilever into the photodiodes, where the signals are then collected and analyzed. When the cantilever is at equilibrium each photodiode receives an equal amount of laser light. However, when the cantilever is deflected due to forces between the probe and the surface, one photodiode collects more light than the others, resulting in an output signal that reflects the angular displacement of the cantilever.

Unfortunately, scan rates for most AFM machines are slow and the time frame for scanning an area the size of a typical protein or DNA molecule can be 30 seconds or more (Visnapuu, Duzdevich et al. 2008). This renders scanning nearly useless for observing real time interactions but very valuable for studying interactions that have been frozen in time, such as DNA wrapping due to transcription by *E. coli* RNA polymerase that have been stalled at predetermined sites (Rivetti, Codeluppi et al. 2003).

When not used for scanning purposes AFM can be used to study properties of single molecules that are attached to the probe end by nonspecific adsorption. Typically, the cantilever is brought into contact with the free end of the molecule and pressed downward to achieve this connection, which can then withstand load forces in the range of 10 – 1000 pN but can sometimes "result in unknown and uncontrolled attachment geometry" (Greenleaf, Woodside et al. 2007). The deflection of the cantilever can be modulated by an active feedback mechanism involving piezoelectric actuators that moves the surface in order to keep the deflection constant, resulting in an unchanging force on the molecule being studied, a scenario that has been used to observe the folding and unfolding pathways of proteins such as polyubiquitin (Fernandez and Li 2004). However, force-extension curves can also be generated if the cantilever is not kept at a constant deflection meaning a change in the surface height results in a change in tension, and extension, of the molecule. This technique has been used to study the extension and unfolding of many different proteins such as titin (Li, Linke et al. 2002) and spectrin (Rief, Pascual et al. 1999).

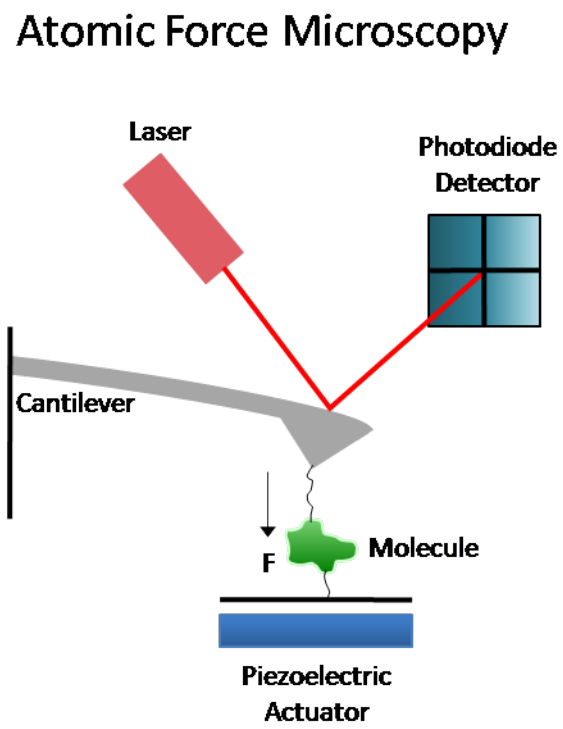

Figure 5: Atomic force microscopy experimental setup. A flexible cantilever with a small probe at the end is scanned over a surface. The probe experiences a repulsive or attractive force whenever it comes into contact with something attached to the surface and the cantilever is deflected. The deflection is measured by a laser and photodiode detector.

1.5 Optical Tweezers (OT)

Optical tweezers use a tightly focused laser to "trap" a bead, usually made out of a dielectric material, inside a tightly focused beam of light. The force on the bead, $F = \alpha \nabla I_0$, is proportional to the gradient of the light intensity, I_0, and the polarizability of the bead, α, but it is also equivalent to a simple mass-spring system, $F = k\Delta x$. In this situation, Δx is the displacement of the bead from the center of the beam and k, the spring constant, is calculated by calibrating the system using the frequency spectrum of the Brownian motion of the bead. The bead is kept in place through a combination of the electric field gradient inside the beam, which attracts the bead towards the area of strongest electric field, and scattering forces generated by absorption and reradiation of light striking the bead (Neuman and Block 2004). Since the forces on the bead, which are generally between 0.1 – 100 pN (Greenleaf, Woodside et al. 2007), depend on the laser

intensity, it is possible to hold the bead at a fixed position with an active feedback mechanism that controls the beam intensity (Visnapuu, Duzdevich et al. 2008). When using optical tweezers, forces are calculated by measuring the displacement of the bead from the center of the beam through a number of techniques such as back-focal-plane detection, where intensity shifts in the laser light at the back focal plane of the lens is measured, and optical interferometry, in which the superposition of scattered and unscattered laser light creates interference patterns that gives nanoscale position measurements of the bead.

Three of the most common and simple geometrical configurations used in optical tweezer experiments are the surface-attached assay, micropipette/single laser trap dumbbell assay, and the double laser trap dumbbell assay. The surface-attached assay setup, in which one end of the molecule is attached to a bio-friendly surface and the other end to a bead in a laser trap, is the simplest geometrical configuration out of the three. However, it suffers from a drifting problem due to laser fluctuations and stage movement that can distort position measurements, a problem that can be remedied by measuring the position of the laser trap relative to the surface, along with the bead position, to compensate for external influences. The second optical tweezer setup, the single laser trap dumbbell, avoids the use of a bio-friendly surface by attaching beads to both ends of the molecule, holding one in position with a micropipette while trapping the other with a laser. This setup offers the advantage of greater molecule maneuverability and increased position tracking, yet still suffers from the same drifting problem as the surface-attached assay, this time due to the mechanical connection to the micropipette. If the micropipette is replaced with a second optical trap – the double trap dumbbell assay – the noise resulting from the mechanical connections of the previous two setups is greatly reduced, though laser position fluctuations due to currents in the surrounding medium become much more significant and must be taking into account.

Though extremely useful for single molecule assays, one precaution that needs to be taken before conducting experiments is the selection of the laser wavelength used to trap the beads. In the past, the use of certain wavelengths of light in optical tweezer experiments proved harmful to biological specimens, so a careful examination of wavelength versus photodamage was conducted in 1999 (Neuman, Chadd et al. 1999) to determine which near-infrared wavelengths were least damaging for single *E. coli* cells. Photodamage was a minimum at 830 and 970 nm and a maximum at 870 and 930 nm (Neuman, Chadd et al. 1999) for *E. coli* cells and the study illuminated the need for the careful selection of lasers and calibration of experimental methods for optical tweezers experiments.

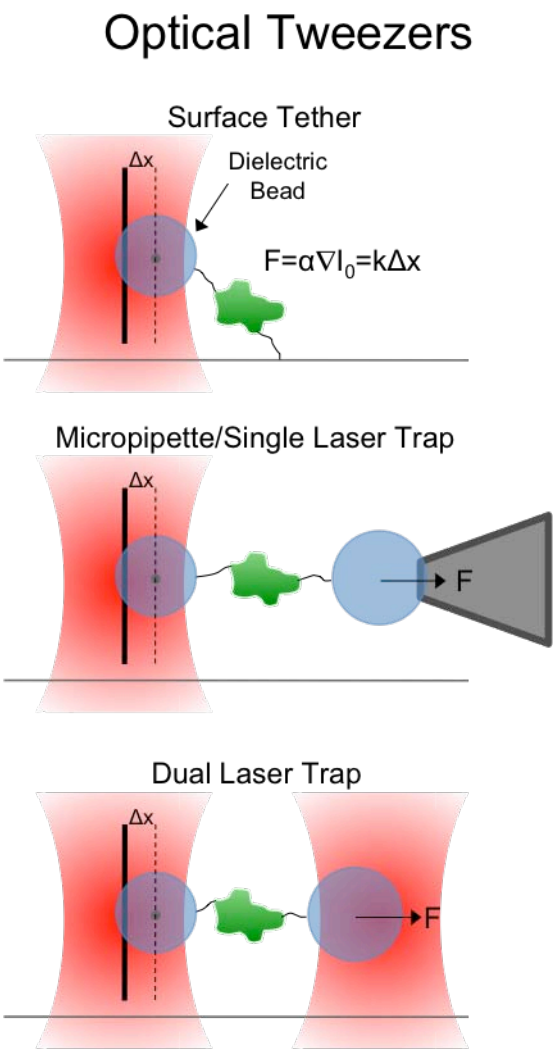

Figure 6: Optical tweezers measure forces on molecules by trapping a dielectric bead in a focused laser beam and measuring the displacement of the bead from the center. The restoring force on the bead is proportional to the gradient of the intensity of the beam. Three common trap setups are the surface tether, the micropipette/single laser trap, and the dual laser trap.

1.6 Magnetic Tweezers (MT)

When a paramagnetic material is placed in a magnetic field it becomes magnetized and experiences a force proportional to the gradient of field, $F = \mu \nabla B$, where μ is the magnetic moment of the paramagnetic material. It is this property of paramagnets that form the basis for the single molecule manipulation technique known as magnetic tweezers (MT). In general, a superparamagnetic bead is attached to the free end of a tethered molecule, which can then be precisely twisted or moved vertically and laterally. Unlike atomic force microscopy, magnetic

tweezers do not require active feedback methods to maintain the position of the bead because the "molecular motions are small compared with the length scale for changes in the field" (Greenleaf, Woodside et al. 2007). This means that once the magnetic field has been established, the force on the bead remains constant. Calculation of the force is based upon the Brownian motion of the bead, with the lateral motion measured by centroid tracking and the vertical motion calculated by analyzing the Airy diffraction pattern produced at certain heights (van Oijen 2007). Though the applicable force range for magnetic tweezers is much smaller than that of AFM, between 0.05 – 20 pN (Greenleaf, Woodside et al. 2007), it allows for much greater control of the molecule and the production of large torque. In a 2002 paper Grosse and Croquette introduced a magnetic tweezers setup that allowed for measurement of the vertical position to within distances of 10 nm, with the lateral positions being even more accurate (Gosse and Croquette 2002).

Applications for magnetic tweezers are far ranging and include the calculation of the persistence length of dsRNA from force-extension curves (Abels, Moreno-Herrero et al. 2005), the discovery that translocation by FtsK, which is essential to cell division, is sequence independent (Saleh, Perals et al. 2004), and the use of torque to wind and unwind DNA to study supercoiling (Strick, Allemand et al. 1998). Though magnetic tweezers are able to apply a very large torque compared to other single molecule manipulation setups (proportional to the magnetic field B) they can only apply forces perpendicular to the surface that are proportional to ∇B. However, magnetic tweezers have the advantage of avoiding the use of potentially molecule damaging lasers and cantilever probes, while requiring relatively simplistic instrumentation.

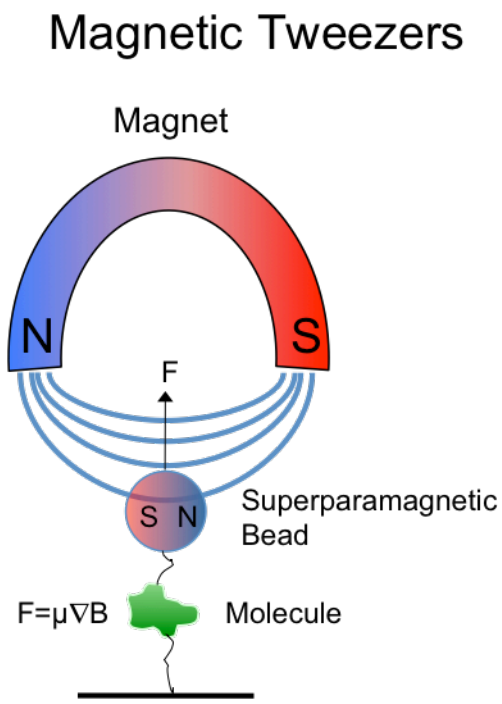

Figure 7: Magnetic tweezers work by creating a strong magnetic field in the region of a superparamagnetic bead that is attached to one end of a tethered molecule. The bead becomes magnetized and experiences a force proportional to and in the direction of increasing magnetic field gradient. Though the gradient may be small, resulting in low linear forces, torsional forces depend on the magnitude of the magnetic field, making magnetic tweezers ideal for twisting molecules.

1.7 Plasmid digestion for long DNA strand amplification

The vast majority of single molecule DNA experiments conducted to date have used λ DNA as the template molecule on which to conduct research (Tanner, Hamdan et al. 2008). λ DNA is the 48,490bp genome of the λ phage, a virus that attacks *Escherichia coli* cells. Along with being commercially available, the entire sequence is well characterized and the contour length is 16.49μm (each base pair is 3.4Å in length, with 1Å = 0.1nm), allowing researchers to easily perform experiments that require a large range of piconewton scale forces. However, there has been a recent surge of interest in the creation of DNA molecules that are not commercially available and are of much shorter lengths than λ DNA for the purpose of studying real time DNA and protein interactions in a much more intimate setting. These smaller fragments are also of

interest because of the vast number of overhang sequences than can be created at their ends to which proteins, fluoropolymers, three way junctions, or other specialized DNA sequences can be attached. Recent studies have focused on using PCR as the sole amplification technique for DNA sizes ranging from 6.7kb to 18kb (Chan, Ha et al. 2006) as well as smaller fragments (~550bp) with unknown sequences (Nakano, Komatsu et al. 2005). PCR, known fully as polymerase chain reaction, is a technique that uses multiple cycles of repeated heating and cooling to denature, anneal, and extend DNA, resulting in an exponential growth of product. However, PCR operates under the constraint of the limited amount of dNTP, the building blocks of DNA strand synthesis, allowed in solution, rendering the process inefficient unless multiple reactions are run at a time, a process that quickly becomes expensive. Also, Taq polymerase, a commonly used enzyme that helps create the hydrogen bonds between nucleotides during synthesis, suffers from an error rate of 1 in 9000 nucleotides synthesized, resulting in nucleotide pairs with no hydrogen bond between them, altering the sequence of the DNA strand.

This experiment uses the techniques of cloning and transformation to amplify an 11kb segment of λ DNA, created initially by PCR, to produce a highly concentrated purified DNA product with a KasI 5' sticky overhang (5'-CTAG-3') on one end and an NheI 5' sticky overhang (5'-CTAG-3') at the other, altogether avoiding the problems of inefficiency, low concentration, and incorrect overhang sequences associated with using only PCR amplification. The 11kb fragments were cloned into the vector pUC19, precut at the BamHI restriction site, to form a circular molecule. The primers used in the initial PCR were chosen so that the overhangs on the 11kb fragment were complementary to the overhangs created at the BamHI cut site on pUC19. The 11kb/pUC19 molecules, referred to as plasmids, were then transformed into *E. coli* cells, which were cultured to form colonies. These colonies were removed, further cultured, and the amplified plasmid removed. The 11kb section of DNA could then be released by digestion with NheI and KasI restriction enzymes and finally purified.

The beauty of this technique revolves around the fact that any cell cultures that grew on our plate and remained white to the eye must have contained the 11kb fragment with our desired overhang sequences. This is because the pUC19 vector contains a gene resistant to ampicillin, an antibiotic that we included in the medium used to culture the *E. coli* cells. Had the plasmid not been transformed into the *E. coli* cells, they would have been killed by the ampicillin on the plate. Thus, the ampicillin guaranteed that any cell colonies that appeared contained at the very least the pUC19 vector. We were also able to avoid colonies containing only pUC19 and not the 11kb fragment, that is, *E. coli* cells with only self-ligated pUC19, by using the sugar X-gal. If the pUC19 had indeed self-ligated a particular gene that had been initially destroyed by the BamHI cut site would have reformed. This gene gives pUC19 the ability to digest X-gal, turning all colonies with self-ligated vectors a blue color. Therefore, since we had eliminated all colonies that could not have contained the plasmid, we knew that the remaining colonies held the 11kb fragment we desired. Though we only performed the plasmid digestion method for one DNA fragment size, we theorize that the technique will work for all DNA lengths, though as the size increases, so too will the complexities of the transformation. However, once the plasmid has been successfully transformed into an *E. coli* cell it can be stored and amplified indefinitely without the need to perform the PCR, cloning, or transformation steps again.

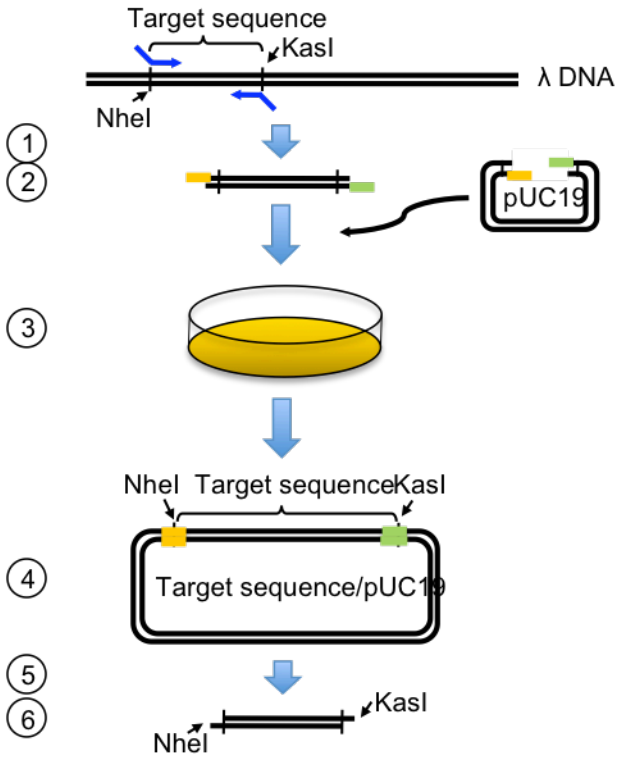

Figure 8: Schematic illustration of the plasmid digestion technique used in this experiment. First the 11kb DNA fragment is amplified at the NheI and KasI restriction enzyme sites using PCR (1). The fragment is then cloned into pUC19, a circular vector precut at the BamHI restriction site to form a linear vector (2). The 11kb/pUC19 plasmid is transformed into *E. coli* cells that are cultured (3) and the plasmid amplified and extracted (4). The 11kb fragment is released from the plasmid by NheI/KasI digestion (5) and purified through gel electrophoresis and extraction (6).

1.8 Adaptor DNA end-labeling

Though sequence specific ligation of adaptor DNA modified by, for example, quantum dots, biotin, or digoxigenin, is not a new concept (Xu, Zhang et al. 2001; Crut, Geron-Landre et al. 2005), it is a process that is plagued by inefficiency. Due to the fickle nature of the PCR process, much of the amplified DNA product may contain the wrong nucleotide sequences on the overhangs, resulting in extremely low yields of successfully modified DNA after the adaptor DNA ligation reaction. Though past studies have claimed up to a 95% yield rate for DNA molecules with two attached adaptor DNA fragments, the mean density of DNA molecules measured on the viewing surface was only around $10^3/mm^2$ and approximately 1% of those

molecules were specifically attached to the surface and contained proper ligation of both adaptor DNA fragments (Crut, Geron-Landre et al. 2005). Thus, statistical measurements were conducted with a sample size of 200 or fewer molecules, with each molecule requiring tedious amounts of searching, or "fishing", to locate. However, the cloning and transformation method results in high yield products that are undeniably comprised of our 11kb fragment with double-labeled ends (and by extension, any fragment length and sticky end sequence that the cloning/transformation method is designed to amplify).

One advantage of this method is the low temperature at which the ligation is performed. When using smFRET, the donor and acceptor chromophores are extremely sensitive to temperature. As the temperature increases, the stability of the chromophores decreases, reducing their efficiency and lifetime. However, the ligation in this experiment is done at 4°C, keeping the chromophores stable and their lifetime intact.

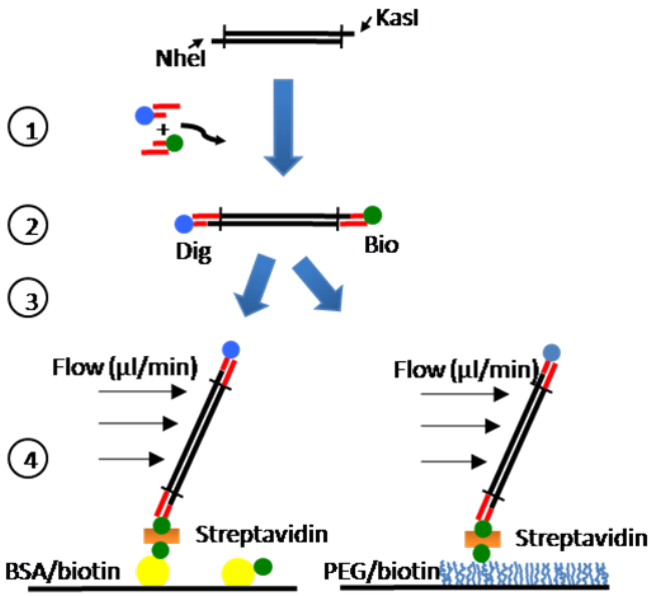

Figure 9: Schematic illustration of the creation and hydrodynamic stretching of digoxigenin/biotion labeled 11kb fragments. First, the single stranded adaptor DNA fragments are annealed to form a double stranded adaptor DNA and ligated at 4°C to the sequence specific sticky ends on the purified 11kb molecule (1). The modified 11kb molecule is then purified to remove any excess DNA ligase or unannealed adaptor DNA fragments (2) and inserted into the BSA or PEG chamber (3). The slide is then washed with fluorescent dye for hydrodynamic stretching experiments (4).

Chapter 2

Results

The main goal of this experiment was to develop a high yield and high efficiency method for amplifying DNA molecules of any size and sequence and to label both ends with the same high yield and efficiency, giving researchers the ability to combine smFRET and force experiments. We performed two different amplification experiments – PCR and plasmid digestion – and measured the concentration of the DNA in solution after each step, using a UV Spectrometer at a wavelength of 260nm (DNA absorbs the maximum amount of light at this wavelength).

For both the PCR and plasmid digestion methods, 0.167nM (in a 100µl volume) of λ DNA was amplified using the forward and reverse primers For-NheI infuse and Rev-KasI infuse (**Table 1**). The solution was then placed in an Eppendorf Mastercycler Personal PCR Machine. The temperature in the machine was raised to 94°C and the solution was incubated for 5 minutes to denature the DNA, followed by 25 cycles of amplification. Each cycle consisted of template denaturization at 94°C for 30 seconds, followed by primer annealing at 50°C for 30 seconds, and extension at 72°C for 11 minutes. After the final cycle the solution was held at 72°C for 1 minute to ensure complete extension.

For the PCR method, the DNA was run on 1% agarose gel and the 11kb fragment was extracted via a gel extraction kit (QIAquick Gel Extraction Kit, Qiagen). The measured concentration after this step was 4.1nM (100µl volume). The NheI (5'-CTAG-3') and KasI (5'-GCGC-3') sticky ends were created during a digestion reaction and the DNA product was purified by the Chroma 1000 spin column kit (Clontech), resulting in a concentration of 2.23nM (120µl volume). Finally, the adaptor DNA was ligated to the sequence specific sticky ends of the 11kb digestion product and purified by the Chroma 100 spin column kit (Clontech). The Chroma spin column series utilize a tube of porous beads to trap DNA fragments below a certain size, allowing all other larger fragments to collect in the bottom of the tube. The final concentration of the adaptor DNA modified 11kb fragment was 1.03nM (150µl volume).

The plasmid digestion method, the procedure for which is explained in Appendix B: Materials and Methods, produced much better results than the PCR method. The concentration of the pUC19/11kb plasmid (110µl volume) after extraction from the cultured *E. coli* cells ranged from 27 – 35nM, a much higher starting value that the 4.1nM concentration of the purified DNA the PCR method began with. After the 11kb molecule was digested from the plasmid, run on 1% agarose gel (**Figure 10**), and purified using the gel extraction kit (Qiagen), the resulting concentration ranged from 7.9 – 11.6nM (concentrated 120µl volume) and 5.2 – 7.35nM (diluted 240µl volume). The drop in concentrate could be due to the fact that a large amount of purified DNA product is not eluted from the extraction kit tube matrices, a problem that can be rectified by washing the tubes with dH_2O multiple times. After the adaptor DNA ligation, the final concentration of modified 11kb DNA ranged from 5.7 – 8.2nM (150µl volume).

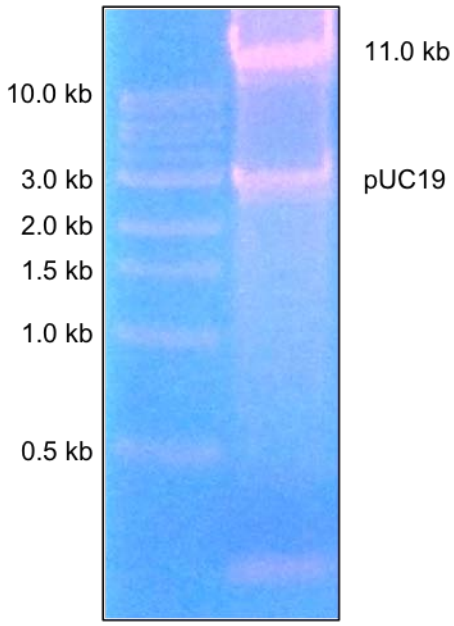

Figure 10: Ethidium Bromide (EtBr) stained 1% agarose gel under a UV lamp. The gel electrophoresis contains the product of the 11kb plasmid digestion. The 11kb band can be clearly seen in the top right while the ~2.7kb linear form of pUC19 can be seen below. The strands on the left come from a template ladder DNA designed to help identify DNA molecules of unknown length.

The modified DNA molecules were inserted into a BSA or PEG coated slide/coverslip (chamber volume of 30-40μl) construct (**Figure 11**) via pipetting at a flow rate of 10μl/min to avoid shearing. After incubating for an hour at room temperature the slide was washed with jojo dye, a molecule that binds to the DNA's backbone and fluoresces under laser light. Hydrodynamic flow experiments were conducted using an inverted Olympus IX-71 microscope that had been modified for total internal reflection (**Figure 12**) experiments using an Nd:YAG laser at 532nm. Fluorescence emission was collected using a water immersion high numerical aperture objective (60x, NA 1.20) and scattered laser light was blocked with a long pass filter (LP 550). Images on the CCD were collected at 30fps and stored as PMA files. An in-house program created in LabView (v8.5, National Instruments) was created that converted the PMA video files into AVI files of any length. The program was also able to average a user selected number of frames from any frame of the PMA file. A threshold was applied to each image, eliminating

pixels below a certain intensity level, and the remaining pixels were isolated according to the size of the diagonal of their bounding rectangle. The size of the diagonal (measured in pixels) was converted to μm (1 pixel = 0.1171875μm) a number that was equal to the extension of the DNA molecule.

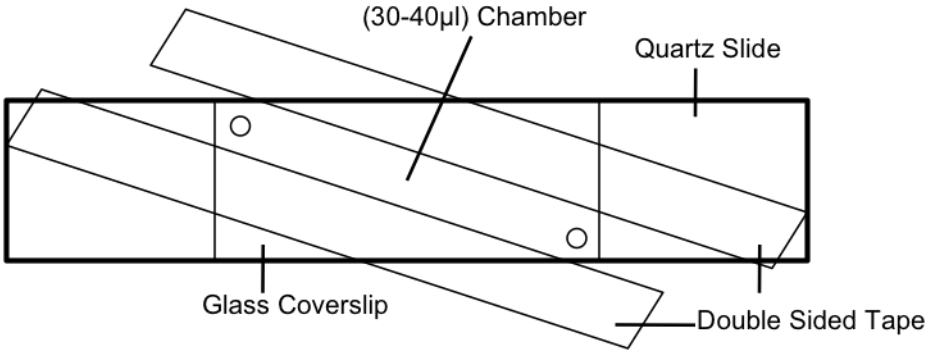

Figure 11: Top view of the BSA/PEG slide construction. The double sided tape is inserted between the coverslip and slide, creating a gap of approximately 100μm and a chamber with a 30-40μl volume. The edges of the slide and coverslip are sealed with epoxy so that air does not enter the chamber when solutions are pushed or pulled through the circular openings.

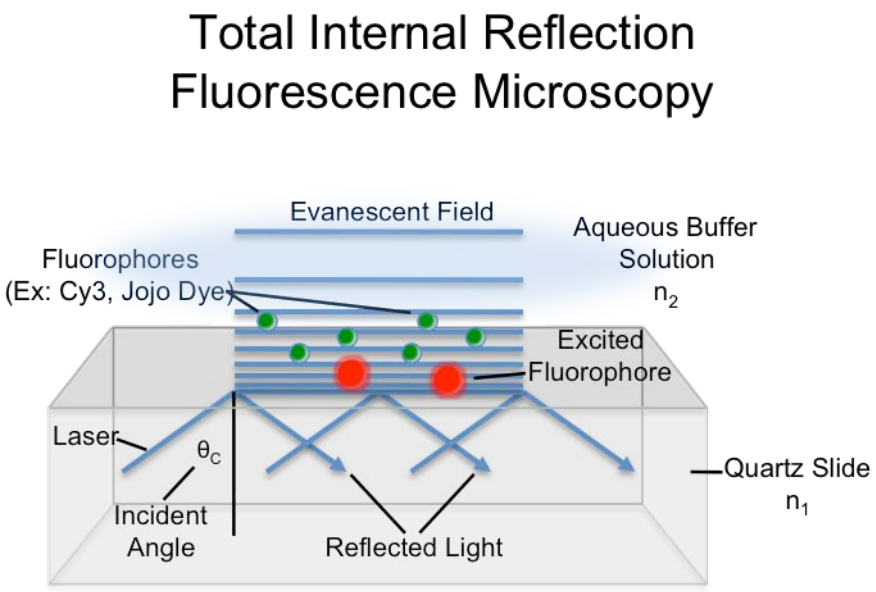

Figure 12: Schematic of total internal reflection microscopy (TIRFM). Laser light enters the quartz slide from a prism (not shown) at an angle greater than the critical angle needed for total internal reflection (also the index of refraction n_1 must be greater than n_2 for total internal reflection to occur). An evanescent field that extends approximately 200nm into the aqueous buffer solution is produced at the interface and excites only fluorophores in that region. TIRFM is extremely useful because it excites the sample in a wide field on the order of 100μm but greatly reduces background fluorescence because of the small penetration depth of the evanescent field.

After the slides had been washed with jojo dye, the surface was examined using the Olympus microscope and TIRFM. Using only 100pM of digoxigenin/biotin labeled DNA on a biotin/streptavidin/BSA surface, over 250 spots per frame fluoresced when there was no buffer flow (**Figure 13, left**). Since the computer displayed a 512x256 (pixel) picture, 250 fluorescing spots corresponded to ~1.5×10^5 spots/mm^2, an extraordinarily high number. However, as mentioned earlier, previous papers found that only around 1% of the spots were specifically bound DNA strands. When buffer was flowed at 100μl/min through the chamber, over 90% of the molecules extended to the same length, indicating that the biotin/digoxigenin labeled DNA had bound with incredibly high efficiency (**Figure 13, right**). In order to test the validity of this number, the flow rate was varied from 20-1000μl/min, holding each flow rate for approximately 5 seconds. The lengths of each DNA strand was measured using the LabView program and plotted against a theoretical force-extension curve for an 11kb DNA fragment with a persistence length

of 52.88nm. As can be seen in **Figure 14**, the data matched up very well with the theoretical curve, deviating slightly above it at lower flow rates. There are two possibilities for this deviation. First, we assumed that there was a linear relationship between the flow rate and force on the DNA molecule. In reality, the flow rate follows more of a parabolic profile, with higher flow rates towards the middle of the chamber, and slower rates at the surfaces. At high flow rates this profile is indeed almost linear, leading to uniform distribution of force along the length of the DNA. However, at low flow rates the profile is decidedly parabolic. This means that the DNA, which is in its coiled form when there is no flow, is stretched by buffer at the surface that is moving significantly slower than we expect, leading to smaller extension measurements.

The second possibility is due to the imaging method used, TIRFM, or total internal reflection fluorescence microscopy. In TIRFM, laser light enters a prism and reflects off of the glass slide at an angle greater than the critical angle, resulting in 100% reflection off of the surface. However, an evanescent field penetrates into the chamber up to 200nm in depth. Any fluorophores within that distance of the surface will become excited and emit light which can be detected by a camera. TIRFM is a particularly useful imaging technique because it reduces the amount of background noise present in images, while offering a wide area of excitation (~1 μm x 1 μm). However, at low flow rates, the DNA does not experience a large force on its length, meaning that part of the strand can extend at a depth greater than 200nm. As such, the Jojo dye attached to the backbone will not be excited by the evanescent field, giving the impression that the DNA is extended less than the force-extension curve predicts.

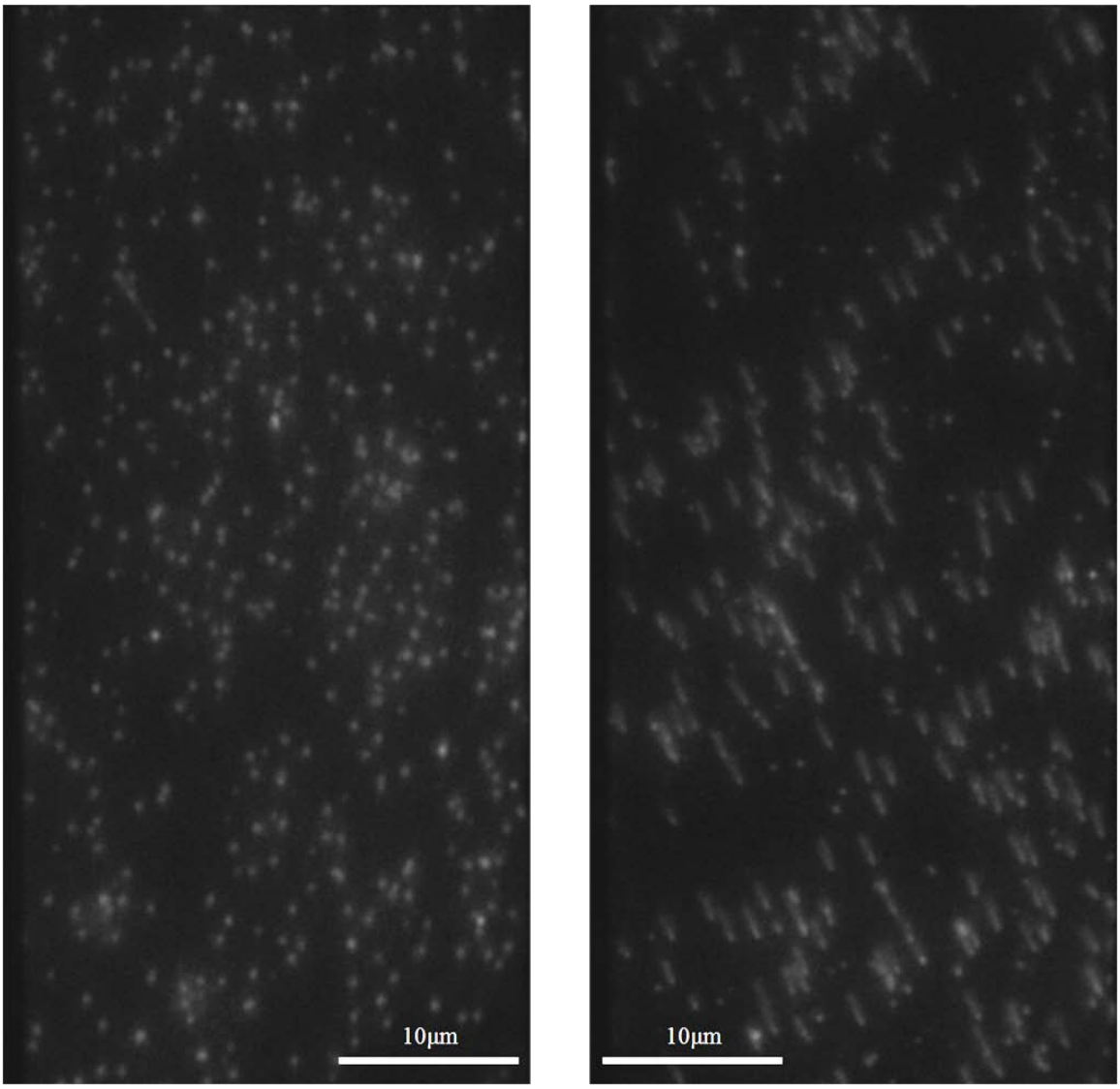

Figure 13: 100pM digoxigenin/biotin labeled jojo dye washed DNA on a biotin/streptavidin BSA surface. With no flow (left) it is impossible to determine how many of the spots are a result of nonspecific binding. However, with 100μl/min flow (right) it becomes clear that the surface is covered with end-labeled 11kb DNA fragments, with mean density ~250/1.7x$10^{-3}$$mm^2$. The white bar represents 10μm and each picture is 60μm in height and 29μm in width.

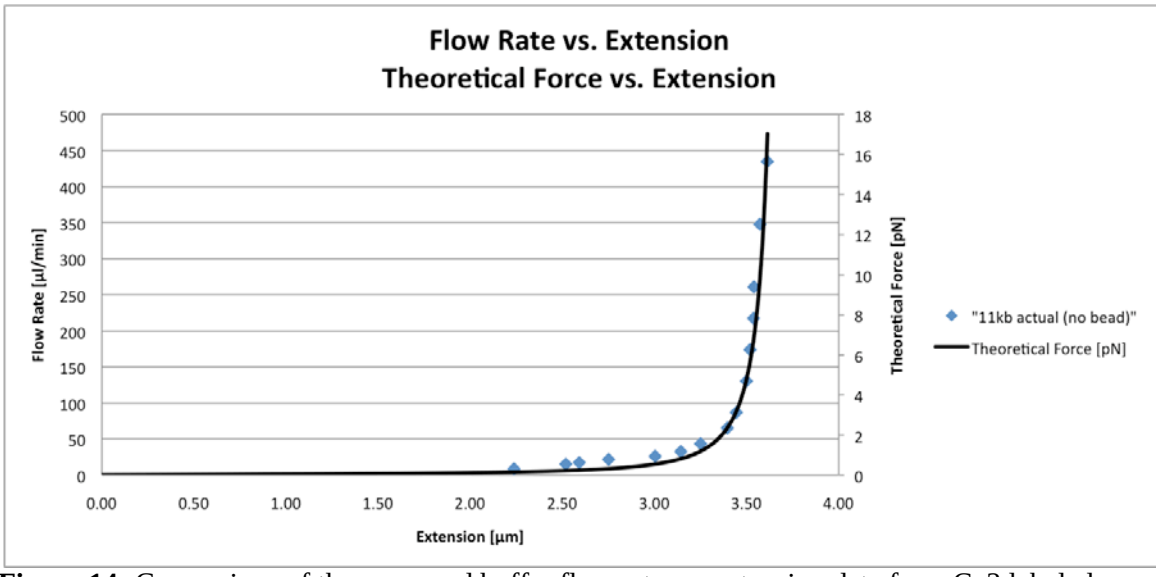

Figure 14: Comparison of the measured buffer flow rate vs. extension data from Cy3 labeled 11kb DNA on a PEG surface to the theoretical 11kb force-extension curve produced using Equation (1). In this case L_0 = 3.74µm, P = 52.88nm, and T = 300K. Extension measurements were made using a LabView program created in-house. Though force-extension measurements have been extensively studied, the graph serves to illustrate the fact that 11kb DNA is indeed specifically bound.

The second test to check if our DNA fragment did indeed have double labeled ends was to attach an antidigoxigenin covered polystyrene bead to a digoxigenin labeled adaptor DNA fragment ligated to the free end of the DNA. We illuminated the beads by scattering light in a light-field microscope, obtaining images with over >250 beads (**Figure 15**), around 70% of which were specifically attached to the DNA (figure not shown). The lateral positions of the beads are calculated by a technique known as Gaussian centroid determination, which can precisely monitor the center of the beads. The mean-square displacement of the Brownian fluctuations of the beads, $\langle \delta\alpha^2 \rangle$, gives precise force measurements by using the equipartition theorem, $F = k_b T l / \langle \delta\alpha^2 \rangle$, where k_b is the Boltzmann constant, T is the absolute temperature, and l is the length of the DNA molecule.

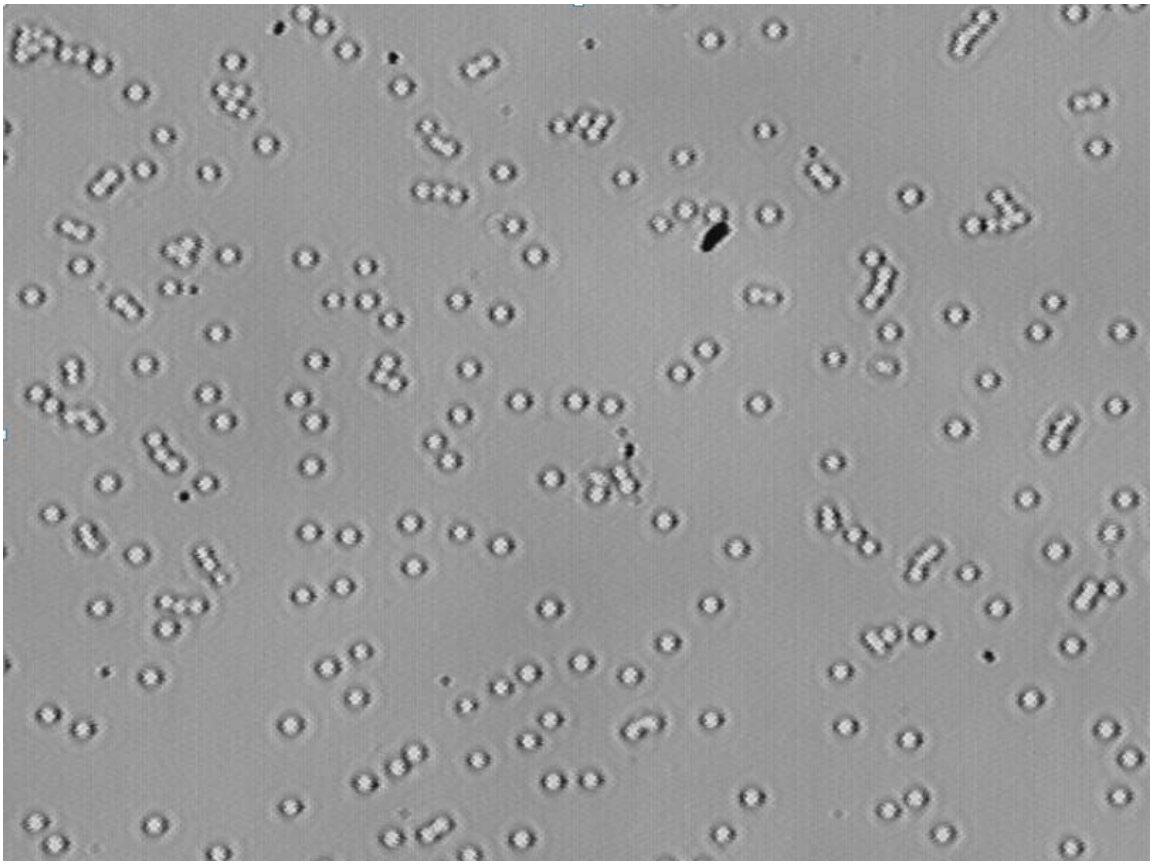

Figure 15: Scattered light in a darkfield microscope illuminates antidigoxigenin coated polystyrene beads which are attached to a digoxigenin labeled adaptor DNA fragment ligated to the free end of the 11kb strand. Over 250 beads are shown in the photo; however, some of them are clustered together, rendering them useless for data collection. When flow is applied (photo not shown), around 70% of the beads "snap" to a new position (a very high efficiency for specific binding). The force applied by the flow can be calculated using the mean-square displacement of the Brownian fluctuations and the equipartion theorem.

Chapter 3

Conclusion and Future Applications

Single-molecule manipulation experiments suffer from inefficient DNA amplification and low density specific binding on bio-friendly slides, resulting in the waste of large amounts of time on finding sufficient quantities of molecules that exhibit desired characteristics on which to conduct statistical analysis. They are also highly challenging from a technical perspective. Traditional amplification techniques such as PCR produce low concentrations of purified DNA, 1.03nM (150µl volume) as we calculated, with no guarantee that any of the product is actually double labeled. Cost is also a factor in PCR amplification, with larger reactions requiring more time and money to complete, again with no guarantee of success. However, this paper demonstrated a technique known as plasmid expression that produced purified DNA product with measured concentrations (150µl volume) of 5.7-8.2nM. The plasmid expression technique not only increased the concentration of the purified DNA but it also guaranteed that the final product was successfully double labeled. Had the DNA molecules not been of the proper length or contained the correct overhang sequences needed for the ligation reaction, the *E. coli* cells would not have even been able to initially grow on the culture plates, meaning that any colonies that did form contained the correct pUC19/11kb plasmid.

Specific adsorption of biotin labeled DNA onto both BSA and PEG surfaces containing a biotin-streptavidin linkage were also much more successful than previous experiments, though PEG slides contained, on average, more molecules than BSA slides. Mean densities of specifically adsorbed DNA molecules were approximately $1.5x10^5/mm^2$, orders of magnitude larger than the *combination* of specific and nonspecific binding mean densities of 10^3-$10^4/mm^2$ seen in PCR amplification alone (Crut, Geron-Landre et al. 2005), where only approximately 1% of the molecules observed contained successfully ligated adaptor DNA fragments. Force-extension data using volumetric flow rates of 20-1000µl/min for biotin/digoxigenin labeled DNA collected using an in-house program written for LabView corresponded to the theoretical force-extension curve for a DNA molecule of length 11kb. This confirms that the DNA is indeed 11kb in length and specifically bound to the surface. In order to test whether or not the DNA is double labeled we attached an antidigoxigenin coated polystyrene bead to the digoxigenin labeled free end of our DNA strand. Using a light-field microscope we observed over 85% specific binding of the bead to the free end, a result that confirms that the DNA is double labeled.

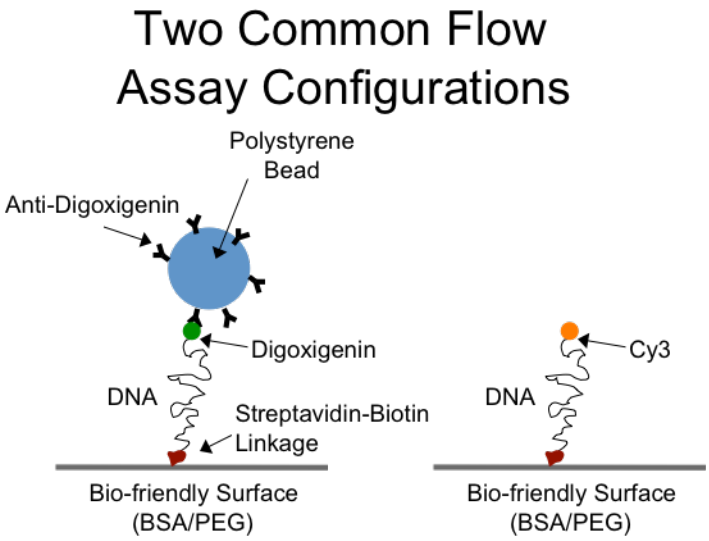

Figure 16: Two common flow assay configurations. These DNA strands are labeled with some of the most basic adaptor DNA configurations: biotin/digoxigenin (left) and biotin/Cy3 (right). However, they can be labeled with more complex configurations such as three-way junctions, Cy3/Cy5 acceptor/donor pairs for smFRET experiments, or hairpin strands. The plasmid digestion method produced extremely large mean densities of specifically bound

biotin/digoxigenin and biotin/Cy3 labeled DNA, leading to the natural assumption that the same will occur for the more complex configurations.

This amplification technique has enormous future potential in multiplexed assays (**Figure 16**), especially for the combination of smFRET and force experiments. FRET is a technique that is used to observe interactions and conformational changes between molecules by monitoring the distance between two neighboring chromophore molecules (a donor, such as Cy3, and an acceptor, such as Cy5) (Clegg 2004). The evanescent field created by TIRFM raises the energy level of the donor chromophore to an excited state, yet does not affect the acceptor chromophore. When the molecules are separated by a distances between 30-80Å, the range where FRET is most effective (Rasnik, Mckinney et al. 2005), the energy of the donor is nonradiatively transferred to the acceptor via an induced-dipole interaction, exciting the acceptor chromophore from its ground state(Clegg 2004)(Rasnik, Mckinney et al. 2005). The efficiency of the energy transfer is given by the equation $E = 1 / [1 + (r / R_0)^6]$, where r is the distance between the donor and acceptor and R_0 is the Förster distance of the donor/acceptor pair, the distance at which the energy transfer efficiency is 50% (not discussed). Looking at the equation, it is clear to see that as the distance between the donor/acceptor pair increases, the energy efficiency transfer decreases. Real time intensity measurements can be made to accurately calculate changes in distance between the donor/acceptor pair using the experimental energy efficiency transfer equation $E = I_A / (I_D + I_A)$, where I_A and I_D are the intensities of the acceptor and donor chromophores, respectively (Rasnik, Mckinney et al. 2005).

Single molecule fluorescence resonance energy transfer (smFRET) experiments, in which the donor/acceptor pair is attached to the same molecule, are able to accurately measure distance changes in the Angstrom range. However, experiments in which force manipulation and smFRET are used at the same time, with the forces being used to simulate system changes in the cell and the smFRET used to measure distance changes much too small for the force experiments alone to

measure, are few and far between. With the technique introduced in this paper, it should now be possible to create a high molecule density surface where a large percentage of molecules contain the chromophores and beads, allowing researchers to avoid “fishing” for suitable molecules on which to conduct their experiments, something that is time consuming and statistically unsound.

In the end, this experiment demonstrated that it is indeed possible to generate long DNA substrates containing asymmetrical ends for high yield and high efficiency double labeling. Hopefully this technique can contribute to the development of effective and stable multiplex array experiments that will allow researchers to combine the angstrom level precision of smFRET with the manipulations controls of force experiments to better understand DNA and its interactions.

Bibliography

Abels, J. A., F. Moreno-Herrero, et al. (2005). "Single-molecule measurements of the persistence length of double-stranded RNA." Biophys J **88**(4): 2737-2744.

Bustamante, C., Z. Bryant, et al. (2003). "Ten years of tension: single-molecule DNA mechanics." Nature **421**(6921): 423-427.

Bustamante, C., J. F. Marko, et al. (1994). "Entropic elasticity of lambda-phage DNA." Science **265**(5178): 1599-1600.

Chan, T. F., C. Ha, et al. (2006). "A simple DNA stretching method for fluorescence imaging of single DNA molecules." Nucleic Acids Res **34**(17): e113.

Cluzel, P., A. Lebrun, et al. (1996). "DNA: an extensible molecule." Science **271**(5250): 792-794.

Crut, A., B. Geron-Landre, et al. (2005). "Detection of single DNA molecules by multicolor quantum-dot end-labeling." Nucleic Acids Res **33**(11): e98.

Fernandez, J. M. and H. Li (2004). "Force-clamp spectroscopy monitors the folding trajectory of a single protein." Science **303**(5664): 1674-1678.

Gosse, C. and V. Croquette (2002). "Magnetic tweezers: micromanipulation and force measurement at the molecular level." Biophys J **82**(6): 3314-3329.

Greenleaf, W. J., M. T. Woodside, et al. (2007). "High-resolution, single-molecule measurements of biomolecular motion." Annu Rev Biophys Biomol Struct **36**: 171-190.

Kabata, H., W. Okada, et al. (2000). "Single-molecule dynamics of the Eco RI enzyme using stretched DNA: its application to in situ sliding assay and optical DNA mapping." Japanese Journal of Applied Physics Part 1-Regular Papers Short Notes & Review Papers **39**(12B): 7164-7171.

Kim, J. H., V. R. Dukkipati, et al. (2007). "Stretching and immobilization of DNA for studies of protein-DNA interactions at the single-molecule level." Nanoscale Research Letters **2**(4): 185-201.

Kim, S. J., P. C. Blainey, et al. (2007). "Multiplexed single-molecule assay for enzymatic activity on flow-stretched DNA." Nature Methods **4**(5): 397-399.

Lebrun, A. and R. Lavery (1996). "Modelling extreme stretching of DNA." Nucleic Acids Res **24**(12): 2260-2267.

Lee, J. B., R. K. Hite, et al. (2006). "DNA primase acts as a molecular brake in DNA replication." Nature **439**(7076): 621-624.

Li, H., W. A. Linke, et al. (2002). "Reverse engineering of the giant muscle protein titin." Nature **418**(6901): 998-1002.

Marko, J. F. and E. D. Siggia (1995). "Statistical-Mechanics of Supercoiled DNA." Physical Review E **52**(3): 2912-2938.

Nakano, M., J. Komatsu, et al. (2005). "Adaptor polymerase chain reaction for single molecule amplification." J Biosci Bioeng **100**(2): 216-218.

Neuman, K. C. and S. M. Block (2004). "Optical trapping." Rev Sci Instrum **75**(9): 2787-2809.

Neuman, K. C., E. H. Chadd, et al. (1999). "Characterization of photodamage to escherichia coli in optical traps." Biophys J **77**(5): 2856-2863.

Rasnik, I., S. A. Mckinney, et al. (2005). "Surfaces and orientations: Much to FRET about?" Accounts of Chemical Research **38**(7): 542-548.

Rief, M., J. Pascual, et al. (1999). "Single molecule force spectroscopy of spectrin repeats: low unfolding forces in helix bundles." J Mol Biol **286**(2): 553-561.

Rivetti, C., S. Codeluppi, et al. (2003). "Visualizing RNA extrusion and DNA wrapping in transcription elongation complexes of bacterial and eukaryotic RNA polymerases." J Mol Biol **326**(5): 1413-1426.

Saleh, O. A., C. Perals, et al. (2004). "Fast, DNA-sequence independent translocation by FtsK in a single-molecule experiment." EMBO J **23**(12): 2430-2439.

Smith, S. B., Y. Cui, et al. (1996). "Overstretching B-DNA: the elastic response of individual double-stranded and single-stranded DNA molecules." Science **271**(5250): 795-799.

Smith, S. B., L. Finzi, et al. (1992). "Direct mechanical measurements of the elasticity of single DNA molecules by using magnetic beads." Science **258**(5085): 1122-1126.

Stigter, D. and C. Bustamante (1998). "Theory for the hydrodynamic and electrophoretic stretch of tethered B-DNA." Biophys J **75**(3): 1197-1210.

Strick, T., J. Allemand, et al. (2000). "Twisting and stretching single DNA molecules." Prog Biophys Mol Biol **74**(1-2): 115-140.

Strick, T. R., J. F. Allemand, et al. (1998). "Behavior of supercoiled DNA." Biophys J **74**(4): 2016-2028.

Tanner, N. A., S. M. Hamdan, et al. (2008). "Single-molecule studies of fork dynamics in Escherichia coli DNA replication." Nat Struct Mol Biol **15**(9): 998.

van Oijen, A. M. (2007). "Honey, I shrunk the DNA: DNA length as a probe for nucleic-acid enzyme activity." Biopolymers **85**(2): 144-153.

Visnapuu, M. L., D. Duzdevich, et al. (2008). "The importance of surfaces in single-molecule bioscience." Mol Biosyst **4**(5): 394-403.

Xu, H., S. Zhang, et al. (2001). "End-labeling of long DNA fragments with biotin and detection of DNA immobilized on magnetic beads." Mol Biotechnol **17**(2): 183-185.

Appendix A

List of Tables

Table 1: List of oligonucleotides.

Oligonucleotides Used		
Name	**Sequence**	**Purpose**
For-NheI infus	5'-CGG TAC CCG GGG ATC GCT AGC AAT TAA TGT GCA TCG ATT ATC AGC-3'	Primer that creates the NheI restriction enzyme site on the 11kb PCR product for cloning into pUC19
Rev-KasI infuse	5'-CGA CTC TAG AGG ATC GGC GCC TGT TGA TTT GAG TTT TGG GTT TAG-3'	Primer that creates the KasI restriction enzyme site on the 11kb PCR product for cloning into pUC19
MonoJ_r	5'-/5Biosg/CCC ACC GCT CGT CTC AAC TGG G-3'	Short oligonucleotide used in the creation of biotin labeled adaptor DNA
KasI-MonoJr	5'-GCG CCC CAG TTG AGA CGA GCG GT-3'	Long oligonucleotide used in the creation of biotin labeled adaptor DNA
NheI-top	5'-CTA GTG GCG ACG GCA GCG AGG C-3'	Long oligonucleotide used in the creation of digoxigenin labeled and Cy3 labeled adaptor DNA
Dig-11kb	5'-/5DigN/GCC TCG CTG CCG TCG CCA-3'	Short oligonucleotide used in the creation of digoxigenin labeled adaptor DNA
Cy3-11kb	5'-/5Cy3/GCC TCG CTG CCG TCG CCA-3'	Short oligonucleotide used in the creation of Cy3 labeled adaptor DNA

Table 2: The two restriction enzymes used to digest the amplified fragment from the 11kb/pUC19 plasmid after it had been extracted from the cultured *E. coli* cells.

Restriction Enzymes	
Enzyme	**Recognition Site**
NheI	pUC19 ← 5’… G ▼C T A G C …3’ → 11kb DNA 3’… C G A T C ▲G …5’
KasI	11kb DNA ← 5’… G ▼G C G C C …3’ → pUC19 3’… C C G C G ▲G …5’

Table 3: Adaptor DNA fragments used in this experiment for conducting specific binding measurements of our modified 11kb molecule.

Adaptor DNA	
Name	**Double Helix Sequence**
Cy3 Adaptor DNA	5’-/5Cy3/ G C C T C G C T G C C G T C G C C A -3’ 3’- C G G A G C G A C G G C A G C G G T G A T C -5’
Biotin Adaptor DNA	5’- G C G C C C C A G T T G A G A C G A G C G G T -3’ 3’- G G G T C A A C T C T G C T C G C C A C C C /5Biosg/-5’
Digoxigenin Adaptor DNA	5’-/5DigN/ G C C T C G C T G C C G T C G C C A -3’ 3’- C G G A G C G A C G G C A G C G G T G A T C -5’

Appendix B

Materials and Methods

PCR

The first step in the experiment, the cutting of the λ DNA (New England Biolabs, Ipswich, MA) to isolate the 11kb fragment of interest, which was then amplified by PCR, followed the protocols given by the MasterAmp Extra-Long PCR Kit (Epicentre Biotechnologies, Madison, WI). A 50µl solution designed to amplify the 11kb fragment and create the NheI and KasI restriction enzyme sites was produced, consisting of 21µl purified H_2O, 25µl Buffer (2x) #9, 1µl Taq polymerase (New England Biolabs, Ipswich, MA), 1µl λ DNA (10ng/µl), 1µl For-NheI infuse primer (100pM), and 1µl Rev-KasI infuse primer (100pM). The solution was then placed in an Eppendorf Mastercycler Personal PCR Machine. The temperature in the machine was raised to 94°C and the solution was incubated for 5 minutes to denature the DNA, followed by 25 cycles of amplification. Each cycle consisted of template denaturization at 94°C for 30 seconds, followed by primer annealing at 50°C for 30 seconds, and extension at 72°C for 11 minutes. After the final cycle the solution was held at 72°C for 1 minute to ensure complete extension and then stored at 4°C until further use.

Cloning and Transformation

The amplified 11kb DNA fragment was then cloned into a linearized vector using the In-fusion Advantage PCR Cloning Kit (Clontech, Mountain View, CA). First, 2µl of Cloning Enhancer (In-fusion Advantage PCR Cloning Kit) was added to 5µl of unpurified 11kb PCR product. The solution was then incubated at 37°C for 15 minutes and at 80°C for another 15 minutes in an Eppendorf Mastercycler Personal PCR Machine. If needed, the Cloning Enhanced PCR product could be stored at -20°C until further use.

When the Cloning Enhanced PCR product was ready, 5µl was added to 2µl of 5x In-fusion Reaction Buffer (In-fusion Advantage PCR Cloning Kit), 1µl of In-Fusion Enzyme (In-fusion Advantage PCR Cloning Kit), and 2µl of linearized vector pUC19 (2,686bp) (In-fusion Advantage PCR Cloning Kit), precut at the BamHI restriction site, for a total volume of 10µl. The reaction was then incubated in an Eppendorf Mastercycler Personal PCR Machine at 37°C for 15 minutes, then at 50°C for 15 minutes, and put on ice when the incubation finished. While on ice, 40µl of TE buffer (10mM Tric-HCl, 1 mM EDTA, pH 8.0) was added to dilute the solution to a total of 50µl. If not used immediately to transform the cells, the cloning reaction can be stored at -20°C.

Once ready to perform the transformation, 2.5µl of the diluted 50µl volume was added to 50µl of competent *E. coli* cell glycerol stock and incubated on ice for 30 minutes. The solution was then placed in a 45°C water heat shock for 45 seconds, enabling the plasmid to enter into the *E. coli* cell, and subsequently placed immediately on ice for 2 minutes to seal the cell walls. 500µl of SOC medium (see page 7 of the In-fusion Advantage PCR Cloning Kit User Manual for SOC medium creation instructions) was added to the plasmid containing *E. coli* solution, which was then shaken for 1 hour at 37°C.

The solution was then spread onto a plate covered in an ampicillin (AMP), bromo-chloro-indolyl-galactopyranoside (X-gal), isopropyl β-D-1-thiogalactopyranoside (IPTG) medium. The pUC19 vector contains an AMP resistant gene, so only *E. coli* cells that included the vector will

have survived on the plate. Any colonies that contained self-ligated pUC19 vectors (no 11kb insert) appeared blue due to the digestion of X-gal by a gene whose sequence was initially broken when pUC19 was cut at the BamHI restriction site, but reformed after the self-ligation. However, all other colonies are assumed to contain the vector and 11kb insert. These colonies were then prepared for plasmid extraction. Using a toothpick, colonies were scraped from the plate and placed into a 10ml solution of LB (Luria-Bertani) medium (pH 7.0) and AMP (10μg/μl), which was then placed in a shaker and incubated overnight at 37°C. The cells could then be used the next day or stored at -20°C until needed.

Plasmid Extraction

The extraction of the plasmid (pUC19 vector with the 11kb insert) from the *E. coli* cells followed the Plasmid DNA Purification with a Microcentrifuge protocol given in the QIAprep Spin Miniprep Kit (Qiagen, Valencia, CA). The pelleted *E. coli* cells were resuspended in 250μl Buffer P1 (Qiagen) by gentle mixing until no cell clumps remained then transferred to a 1.5ml microcentrifuge tube. 250μl of Buffer P2 (Qiagen) was added to the tube, which was then slowly inverted 5 times to ensure the solution was thoroughly mixed. The combination of Buffer P1 and Buffer P2 induces the breaking down, or lysis, of the *E. coli* cell and was allowed to proceed for ~4.5 minutes at room temperature, though not longer than 5 minutes. 350μl of Buffer N3 (Qiagen) was then added and each tube was mixed immediately until the solution attained a cloudy appearance.

Each tube was then centrifuged in a table-top microcentrifuge for 10 minutes at 13,000 rpm, (~17,900 x *g*). After this stage, the tubes contained a compact white pellet and supernatants containing the unpurified plasmid. The supernatants were then applied to a QIAprep spin column (QIAprep Spin Miniprep Kit), which is designed to retain high-copy plasmid DNA, via pipetting. The spin column was centrifuged for 1 minute and the flow-through, containing excess buffer and

cell material from the initial protocol steps, was discarded. The spin column was then washed with 0.5ml Buffer PB (Qiagen) and centrifuged for 1 minute to remove any trace nuclease activity. After discarding the flow-through the spin column was washed with 0.75ml Buffer PE (Qiagen) and centrifuged for 1 minute. The flow-through was discarded and the spin column was centrifuged again for 1 minute to remove any excess buffer. The spin column was placed in a fresh 1.5ml microcentrifuge tube and 30µl of dH_2O was added to the center of the spin column. The column and tube were centrifuged for 1 minute to elute the plasmid, which collected in the centrifuge tube. This process could be repeated as many times as needed to dilute the plasmid to a desired volume. The purified plasmid solution was then stored at -20°C until further use.

Digestion from Plasmid

The concentration of the plasmid solution was necessary to determine the volume of reactants needed to release the 11kb fragment by digestion. The concentration was calculated using the absorbency of a 20x plasmid solution dilution at a wavelength of 260nm, which was generated by a UV Spectrometer. The relationship between the absorbency and the concentration of the DNA is governed by the following equation:

$$c = A_{260} * D * 0.05 \tag{3}$$

where c is the concentration of the DNA in µg/µl, D is the dilution factor (20 in this specific case), and A_{260} is the absorbency of the DNA at a wavelength of 260nm. The total amount of DNA in the sample is given by:

$$Y = c * V_p \tag{4}$$

where Y is the DNA yield in µg and V_p is the total plasmid volume in µl.

After establishing a baseline correlation over a wavelength range of 250 – 270 nm using 100µl of dH_2O, a 20x dilution of 5µl plasmid solution and 95µl dH_2O was scanned over the same range to find the value of A_{260nm}. The molarity of the plasmid solution was typically in the range of 25 – 40nM and was calculated by dividing the concentration by the molecular weight of the plasmid, which is 8,474,282Da.

Once the concentration of the plasmid solution was calculated it became possible to set up the digestion reaction to release the 11kb fragment. The reaction utilized two enzymes, KasI (New England Biolabs) and NheI (New England Biolabs) to cut the 11kb fragment at the exact sequences that were digested during the initial PCR step. The plasmid, Buffer #2 (New England Biolabs) - used to improve the efficiency of the NheI/KasI digestion - and dH_2O comprised the other elements in the reaction. According to New England Biolabs, in a 50µl volume, 1µl of restriction enzyme can digest 1µg of DNA in an hour when the tube containing the volume is incubating at 37°C. However, when using Buffer #2, NheI can digest 1µg of DNA in 15 minutes. In general, a total volume of 200µl was desired with 5µl each of KasI and NheI, 20-30µl Buffer #2, 50-100µl plasmid – depending on the concentration – and the remaining volume made up of dH_2O. Once all the components were added the microcentrifuge tube was immersed in a water bath and incubated at 37°C overnight to ensure the maximum amount of plasmid was digested.

Electrophoresis and Gel Extraction

When the digestion was complete the contents of the microcentrifuge tube were run on 1% Agarose Gel (75µl 1xTBE Buffer, 0.75g Agarose) using a 6 well gel electrophoresis to separate the different lengths of DNA created by the digestion. To visualize the progress of the electrophoresis, 50 - 60µl of 6x DNA Loading Dye (Fermentas) was added to the digestion product, which was then divided equally among 5 of the 6 wells. The sixth well was filled with 5µl of 6x DNA Loading Dye (Fermentas) and 1.5µl of 1kb DNA Ladder (New England Biolabs) to use as a control when identifying the digestion DNA fragment sizes. The electrophoresis was

run for approximately 1 hour and then the gel was soaked in Ethidium Bromide (EtBr) for 45 minutes to stain the DNA, which then fluoresced when exposed to ultraviolet light. The gel contained 2 distinct bands that corresponded to the 11kb fragment and the pUC19 vector, along with a faint band at 182b (KasI not only cuts the 11kb fragment but also cuts pUC19 at the 235b site which is 182b from the BamHI cut site).

Once the 11kb band was identified it was cut out of the gel and purified using the QIAquick Gel Extraction Kit (Qiagen). The gel containing the fragment was chopped into smaller pieces, placed in a 15ml tube with 5ml of QG buffer (Qiagen), and incubated in a water bath at 50°C until the gel had completely dissolved. Equal amounts of solution was applied to four Qiagen spin columns and centrifuged at 13,000 RPM for 1 minute. The flow-through was discarded and the step repeated until the sample was completely finished. 500µl of QG buffer (Qiagen) was added to each of the 4 spin columns, which were then centrifuged for 1 minute at 13,000 RPM to remove any residual Agarose Gel. After the flow-through was discarded, 750µl of PE Buffer (Qiagen) was added and the spin columns were once again centrifuged for 1 minute at 13,000 RPM. A final 1 minute centrifuge was necessary to completely remove the PE buffer from the spin column.

After the PE buffer has been removed each spin column was placed in a new 1.5ml microcentrifuge tube and 20µl of dH_2O was applied to the center of the sample and the tube was centrifuged at 13,000 RPM for 1 minute to elute the DNA. This step was repeated until each of the 4 tubes contained 60µl of samples. Two of the tubes were collected and combined to create a concentrated 11kb sample, while the other two were centrifuged to a volume of 120µl each and combined to create a dilute 11kb sample. The absorbency of both the dilute and concentrated samples was measured and the concentration calculated. The molarity, typically in the range of 8-20nM of each was calculated by dividing the concentration by the MW, 6,800,141Da, of the 11kb fragment. The purified samples could then be stored at -20°C if needed.

Creation of Adaptor DNA and 11kb Fragment Ligation

10nM of biotin labeled adaptor was prepared by hybridizing a long oligonucleotide, KasI-MonoJr, and a short oligonucleotide, MonoJ_r, at a 2:3 molar ratio to create a KasI 5' sticky overhang (5'-GCGC-3'). Also, 10nM of digoxigenin labeled adaptor was prepared by hybridizing at a 2:3 molar ratio long oligonucleotide, NheI-top, and a short oligonucleotide, Dig-11kb to create NheI sticky end (5'-CTAG-3'). Depending on the experiment the short oligonucleotide, Dig-11kb, could be replaced by a Cy3 labeled short oligonucleotide, Cy3-11kb, to create a Cy3 labeled adaptor DNA with the same NheI sticky end as the digoxigenin labeled fragment. Each reaction was heated to 80°C for 3 minutes in an Eppendorf Mastercycler Personal PCR Machine then allowed to cool down to room temperature over a period of 2-3 hours to complete the annealing of the long and short oligonucleotides.

The ligation reaction setup depended on the concentration of the purified 11kb fragment volume created in the gel extraction step. A final volume of 150µl was desired, which included 15µl of 10x T4 DNA Ligase Buffer (New England Biolabs) and 5µl of T4 DNA Ligase (New England Biolabs) to repair any single stranded holes that are left after the sticky ends are joined. The 11kb fragment was first diluted to a molarity of 10nM. The biotin and digoxigenin/Cy3 adaptor DNA products were both diluted to 5x that of the 11kb fragment (50nM) and 0.5 – 1.0µl of each was added to the solution. The difference between the final desired volume of 150µl and the volume of the adaptor DNA, 11kb fragment, T4 Buffer, and T4 Ligase was made up of dH_2O. The reaction was then incubated at 16°C overnight in an Eppendorf Mastercycler Personal PCR Machine. It is important to note the specific order in which to add the ingredients to the reaction so as to preserve the integrity of the ligase and adaptor DNA: dH_2O → T4 Buffer → 11kb DNA → adaptor DNA → T4 DNA Ligase. The modified DNA product is then purified using the Chroma 100 spin column kit (Clontech). The Chroma spin column series utilize a tube of porous

beads to trap DNA fragments below a certain size, allowing all other larger fragments to collect in the bottom of the tube.

BSA Slides

Starting with a clean, assembled slide, wash the chamber with 100µl T50 buffer. Epoxy the edges of the slide to seal the chamber then wait for the epoxy to completely dry (~10 minutes). Wash the slide again with 100µl T50 buffer to confirm the chamber is sealed properly. Next, add 60µl of 1mg/ml biotinylated BSA in T50 buffer and incubate the slide at room temperature for 10 minutes. Once the slide is finished incubating, wash it once more with 100µl T50 buffer to remove any excess biotinylated BSA. Add 0.25mg/ml streptavidin (3µl of 5mg/ml stock streptavidin and 57µl T50 buffer) and incubate again at room temperature for 10 minutes. Wash the slide again with 100µl T50 buffer and add DNA (20pM – 10nM DNA for specific binding and 1 mg/ml BSA and T50 buffer for a total volume of 60µl). Incubate for an hour to ensure specific binding and wash a final time with 100µl T50 buffer.

PEG Slides

Coating the slides with aminosilane

Organosilanes are compounds containing silicon to carbon bond. Organosilanes can be used to modify a surface. For instance, aminosilane—a specific type of organosilane—can be attached to the surface of a negatively charged quartz slide, and this reaction will result in a ~2nm coating of positively charged, reactive amine groups that can be used for downstream reactions. Using quartz slides and glass coverslips that have been thouroughly cleaned and heated/burned to remove impurities:

1. Using a small Erlenmeyer flask:
    a. Put 100 mL of methanol into the flask.

b. Put 5 mL of purified water into the flask.

c. Put 1 mL of acetic acid into the flask. Make sure you use a glass tip over the plastic tip when you are getting the acetic acid.

d. Put 2 mL of amino-silaine in the flask (use a glass pipet tip for this). This step must be done quickly so that it doesn't oxidize.

e. Seal the aminosilane bottle.

2. Make sure that the mixture in the labeled flask is mixed well by swirling the container.
3. Pour the solution into glassware containing the purified quartz slides and glass coverslips. Put the lids on the glassware. Immediately rinse the Erlenmeyer flask with nanopure water.
4. Put the glassware in the hot bath for 10 minutes.
    a. Place the jar of aminosilane in a vacuum chamber.
        i. Leave the aminosilane bottle in the vacuum chamber for 10 minutes. Make sure the lid on the bottle is loose.
        ii. Fill the vacuum chamber with N_2.
        iii. Open the chamber quickly and tighten the lid on the aminosilane.
        iv. Seal the lid with parafilm.
5. Sonicate the glassware for 1 minute at a temperature of 55°C.
6. Leave the glassware in the hot bath for another 10 minutes.
7. Remove the flasks from the sonicator. At this point the aminosilane solution should be attached to the surfaces.
8. For both the coverslips and the slides:
    a. Dump out the solution.
    b. Rinse two times with methanol.
    c. Rinse many times with purified water.

d. Fill the flasks with purified water.

PEG conjugation

9. Make a sodium bicarbonate buffer ($NaHCO_3$)
    a. Measure of ~84 mg of the $NaHCO_3$ power with a clean spatula.
    b. Put the power in a 15 mL plastic container.
    c. Fill the container up to the 10 mL line with nanopure water.
    d. *Note* You must used the sodium bicarbonate buffer the same day you make it.
10. Using room temperature vials of PEG with and without biotin:
    a. Weigh out 80 mg of the PEG and put it in a 1.5 ml tube.
    b. Weigh out ~3 mg of the PEG with biotin and put it in the 1.5 ml tube.
    c. Put 320 μL of $NaHCO_3$ buffer into the test tube. Flick it. Centrifuge it for one minute. The solution is highly viscous, so the spinning is necessary to eliminate bubbles. After one minute of spinning, you should have a clear solution.
    d. Put the PEG vials in the vacuum for 30 minutes. Break the vacuum with N_2 and quickly close the lids and seal the vials with parafilm.
11. Dry the slides (The quicker the slides and coverslips are prepared, the cleaner they will be.):
    a. Starting with the coverslips:
        i. Rinse coverslips well with purified water.
        ii. Dry the coverslips with filtered air (or N_2).
        iii. Put the coverslips in dry glassware and cover with a lid.
    b. Proceed to the slides:
        i. Rinse the slides well with purified water.
        ii. Dry the slides with filtered air (or N_2).

iii. Lay the slides in an empty container (in this case, a pipette container) and close the lid.

12. Put 70 μL of the PEG solution on top of each slide and put a coverslip over each slide. By this method, both internal surfaces are getting coated by the PEG.
13. Put water in the boxes (though not on the slides) to keep the slides from drying out and put the lids on the boxes. Put the boxes in a dark place so the polymer will not get hydrolyzed by the light.
14. Throw out the $NaHCO_3$ buffer.
15. After 3 hours the PEG slides should be complete and ready for construction.